

Production of the MSSM Higgs Bosons at Next Generation Linear e^+e^- Colliders

A. Gutiérrez-Rodríguez ¹, M. A. Hernández-Ruiz ¹ and O. A. Sampayo ²

(1) *Facultad de Física, Universidad Autónoma de Zacatecas*

Apartado Postal C-580, 98060 Zacatecas, Zacatecas México.

(2) *Departamento de Física, Universidad Nacional del Mar del Plata*

Funes 3350, (7600) Mar del Plata, Argentina.

(November 2, 2018)

Abstract

We study the production of the Higgs bosons predicted in the Minimal Supersymmetric extension of the Standard Model (h^0, H^0, A^0, H^\pm), with the reactions $e^+e^- \rightarrow b\bar{b}h^0(H^0, A^0)$, and $e^+e^- \rightarrow \tau^-\bar{\nu}_\tau H^+, \tau^+\nu_\tau H^-$, using the helicity formalism. We evaluate cross section of h^0, H^0, A^0 and H^\pm in the limit when $\tan\beta$ is large. The numerical computation is done considering two stages of a possible Next Linear e^+e^- Collider: the first with $\sqrt{s} = 500$ GeV and design luminosity $50 fb^{-1}$, and the second with $\sqrt{s} = 1 TeV$ and luminosity $100\text{-}200 fb^{-1}$.

PACS: 14.80.Cp, 12.60.Jv

I. INTRODUCTION

Higgs bosons [1] play an important role in the Standard Model (SM) [2]; they are responsible for generating the masses of all the elementary particles (leptons, quarks, and gauge bosons). However, the Higgs-boson sector is the least tested one in the SM. If Higgs bosons are responsible for breaking the symmetry from $SU(2)_L \times U(1)_Y$ to $U(1)_{EM}$, it is natural to expect that other Higgs bosons are also involved in breaking other symmetries. One of the more attractive extensions of the SM is Supersymmetry (SUSY) [3], mainly because of its capacity to solve the naturalness and hierarchy problems while maintaining the Higgs bosons elementary.

The theoretical frame work of this paper is the Minimal Supersymmetric extension of the Standard Model (MSSM), which doubles the spectrum of particles of the SM and the new free parameters obey simple relations. The scalar sector of the MSSM [4] requires two Higgs doublets, thus the remaining scalar spectrum contains the following physical states: two CP-even Higgs scalar (h^0 and H^0) with $m_{h^0} \leq m_{H^0}$, one CP-odd Higgs scalar (A^0) and a charged Higgs pair (H^\pm), whose detection would be a clear signal of new physics. The Higgs sector is specified at tree-level by fixing two parameters, which can be chosen as the mass of the pseudoscalar m_{A^0} and the ratio of vacuum expectation values of the two doublets $\tan \beta = v_2/v_1$, then the mass m_{h^0} , m_{H^0} and m_{H^\pm} and the mixing angle of the neutral Higgs sector α can be fixed. However, since radiative corrections produce substantial effects on the predictions of the model [5], it is necessary to specify also the squark masses, which are assumed to be degenerated. In this paper, we focus on the phenomenology of the neutral CP-even and CP-odd scalar (h^0, H^0, A^0) and charged (H^\pm).

The search for these scalars has begun at LEP, and current low energy bound on their masses gives $m_{h^0}, m_{A^0} > 90 \text{ GeV}$ and $m_{H^\pm} > 120 \text{ GeV}$ for $\tan \beta > 1$ [6]. At e^+e^- colliders the signals for Higgs bosons are relatively clean and the opportunities for discovery and detailed study will be excellent. The most important processes for the production and detection of the neutral and charged Higgs bosons h^0, H^0, A^0 and H^\pm , are: $e^+e^- \rightarrow Z^* \rightarrow h^0, H^0 + Z^0$,

$e^+e^- \rightarrow Z^* \rightarrow h^0, H^0 + A^0$, $e^+e^- \rightarrow \nu\bar{\nu} + W^{+*}W^{-*} \rightarrow \nu\bar{\nu} + h^0, H^0$ (the later is conventionally referred to as WW fusions), and $e^+e^- \rightarrow H^+H^-$ [7]; precise cross-section formulas appear in Ref. [8]. The main decay modes of the neutral Higgs particles are in general $b\bar{b}$ decays ($\sim 90\%$) and $\tau^+\tau^-$ decays ($\sim 10\%$) which are easy to detect experimentally at e^+e^- colliders [9–11]. Charged Higgs particles decay predominantly into $\tau\nu_\tau$ and $t\bar{b}$ pairs.

In previous studies, the two-body processes of the neutral and charged Higgs bosons $e^+e^- \rightarrow h^0(H^0) + Z^0$, $e^+e^- \rightarrow h^0(H^0) + A^0$ and $e^+e^- \rightarrow H^+H^-$ have been evaluated [8] extensively. However, the inclusion of three-body process with heavy fermions f , $e^+e^- \rightarrow (f\bar{f}h^0, f\bar{f}H^0, f\bar{f}A^0)$, [12,13] and $e^+e^- \rightarrow \tau^-\bar{\nu}_\tau H^+, \tau^+\nu_\tau H^-$ [14,15] at future e^+e^- colliders energies [16–18] is necessary in order to know its impact on the two-body mode processes and also to search for new relations that could have a cleaner signature of the Higgs bosons production.

In the present paper we study the production of SUSY Higgs bosons at e^+e^- colliders. We are interested in finding regions that could allow the detection of the SUSY Higgs bosons for the set parameter space ($m_{A^0} - \tan\beta$). We shall discuss the neutral and charged Higgs bosons production $b\bar{b}h^0(H^0, A^0)$, and $\tau^-\bar{\nu}_\tau H^+, \tau^+\nu_\tau H^-$ in the energy range of a future e^+e^- collider [16–18] for large values of the parameter $\tan\beta$, where one expects to have a high production. Since the coupling $h^0b\bar{b}$ is proportional to $\sin\alpha/\cos\beta$, the cross-section will receive a large enhancement factor when $\tan\beta$ is large. Similar situation occurs for H^0 , whose coupling with $b\bar{b}$ is proportional to $\cos\alpha/\cos\beta$. The couplings of A^0 with $b\bar{b}$ and of H^\pm with $\tau^-\bar{\nu}_\tau, \tau^+\nu_\tau$ are directly proportional to $\tan\beta$, thus the amplitudes will always grow with $\tan\beta$. We consider the complete set of Feynman diagrams at tree-level and use the helicity formalism [19–25] for the evaluation of the amplitudes. Succinctly, our aim in this work is to analyze how much the results of the Bjorken Mechanism [Fig. 1, (1.4)] would be enhanced by the contribution from the diagrams depicted in Figs. 1.1-1.3, 1.5 and 1.6 in which the SUSY Higgs bosons are radiated by a $b(\bar{b})$ quark. For the case of the charged Higgs bosons the two-body mode [Figs. 3.1 and 3.4] would be enhanced by the contribution from the diagrams depicted in Figs. 3.2, 3.3, and 3.5, in which the charged Higgs boson is

radiated by a $\tau^- \bar{\nu}_\tau$ ($\tau^+ \nu_\tau$) lepton.

Recently, it has been shown that for large values of $\tan \beta$ the detection of SUSY Higgs bosons is possible at FNAL and LHC [26]. In the papers cited in Ref. [26] the authors calculated the corresponding three-body diagrams for hadron collisions. They pointed out the importance of a large bottom Yukawa coupling at hadron colliders and showed that the Tevatron collider may be a good place for detecting SUSY Higgs bosons. In the case of the hadron colliders the three-body diagrams come from gluon fusion and this fact makes the contribution from these diagrams more important, due to the gluon abundance inside the hadrons. The advantage for the case of e^+e^- colliders is that the signals of the processes are cleaner.

This paper is organized as follows. We present in Sec. II the relevant details of the calculations. In Sec. III we evaluate cross section for the processes $e^+e^- \rightarrow b\bar{b}h^0(H^0, A^0)$ and $e^+e^- \rightarrow \tau^-\bar{\nu}_\tau H^+, \tau^+\nu_\tau H^-$ at future e^+e^- colliders. Finally, Sec. IV contains our conclusions.

II. HELICITY AMPLITUDE FOR HIGGS BOSONS PRODUCTION

When the number of Feynman diagrams is increased, the calculation of the amplitude is a rather unpleasant task. Some algebraic forms [27] can be used in it to avoid manual calculation, but sometimes the lengthy printed output from the computer is overwhelming, and one can hardly find the required results from it. The CALKUL collaboration [28] suggested the Helicity Amplitude Method (HAM) which can simplify the calculation remarkably and hence make the manual calculation realistic.

In this section we describe in brief the evaluation of the amplitudes at tree-level, for $e^+e^- \rightarrow b\bar{b}h^0(H^0, A^0)$ and $e^+e^- \rightarrow \tau^-\bar{\nu}_\tau H^+, \tau^+\nu_\tau H^-$ using the HAM [19–25]. This method is a powerful technique for computing helicity amplitudes for multiparticle processes involving massless spin-1/2 and spin-1 particles. Generalization of this method that incorporates massive spin-1/2 and spin-1 particles, is given in Ref. [25]. This algebra is easy to program

and more efficient than computing the Dirac algebra.

A Higgs boson h^0, H^0, A^0 , and H^\pm can be produced in scattering e^+e^- via the following processes:

$$e^+e^- \rightarrow b\bar{b}h^0, \quad (1)$$

$$e^+e^- \rightarrow b\bar{b}H^0, \quad (2)$$

$$e^+e^- \rightarrow b\bar{b}A^0, \quad (3)$$

$$e^+e^- \rightarrow \tau^-\bar{\nu}_\tau H^+, \tau^+\nu_\tau H^-. \quad (4)$$

The diagrams of Feynman, which contribute at tree-level to the different reaction mechanisms, are depicted in Figs. 1-3.

However those diagrams with exchange of Higgs bosons instead of gauge bosons (photon or Z^0) have been neglected because of the smallness of the Higgs fermion coupling. Using the Feynman rules given by the Minimal Supersymmetric Standard Model (MSSM), as summarized in Ref. [8], we can write the amplitudes for these reactions. For the evaluation of the amplitudes we have used the spinor-helicity technique of Xu, Zhang and Chang [20] (denoted henceforth by XZC), which is a modification of the technique developed by the CALKUL collaboration [28]. Following XZC, we introduce a very useful notation for the calculation of the processes (1)-(4). The complete formulas of the processes (1)-(3) are given in Ref. [13], while for the case of process (4), are given in Ref. [14]. We are going to use the same notation and the formulas given in [13,14] and do not reproduce them here.

After writing down the Feynman diagrams corresponding to a given amplitude \mathcal{M} an usually proceeds to derive an analytic expression for the cross section $\sum |\mathcal{M}|^2$, with an appropriate spin and/or color sum or average. The result, which is usually a function of Minkowsky products of the particle four-momenta, is then evaluated numerically at phase-space points in the region of interest.

It is clear that any method which evaluates \mathcal{M} instead of $\sum |\mathcal{M}|^2$ will eventually become superior to the standard approach. Indeed, several authors have stressed this point and proposed alternatives.

We want to argue that it is useful to employ in the evaluation of the amplitude not vector products like $p_1 \cdot p_2$ but rather spinor products like $\bar{u}(p_1)u(p_2)$.

After the evaluation of the amplitudes of the corresponding diagrams, we obtain the cross-sections of the analyzed processes for each point of the phase space using Eqs. (12)-(17), (23)-(28) and (11)-(15) [13,14] by a computer program, which makes use of the subroutine RAMBO (Random Momenta Beautifully Organized) [29]. The advantages of this procedure in comparison to the traditional “trace technique” are discussed in Refs. [19–25].

We use the Breit-Wigner propagators for the Z^0 , h^0 , H^0 , A^0 and H^\pm bosons. For the SM parameters we adopted the following: $m_b = 4.25 \text{ GeV}$, $m_t = 175 \text{ GeV}$, $m_\tau = 1.78 \text{ GeV}$, $m_\nu = 0$, $m_{Z^0} = 91.2 \text{ GeV}$, $\Gamma_{Z^0} = 2.4974 \text{ GeV}$, $\sin^2 \theta_W = 0.232$, which are taken as inputs. The widths of h^0 , H^0 , A^0 and H^\pm are calculated from the formulas given in Ref. [8]. In the next sections we present the numerical computation of the processes $e^+e^- \rightarrow b\bar{b}h$, $h = h^0, H^0, A^0$ and $e^+e^- \rightarrow \tau^-\bar{\nu}_\tau H^+, \tau^+\nu_\tau H^-$.

III. PRODUCTION OF THE MSSM HIGGS BOSONS AT NEXT GENERATION POSITRON-ELECTRON COLLIDERS

In this paper, we evaluate total cross section of neutral and charged MSSM Higgs bosons at next generation e^+e^- colliders, including three-body mode diagrams [Figs. 1.1-1.3, 1.5, and 1.6; Figs. 2.1-2.3, 2.5 and 2.6; Figs. 3.2, 3.3, and 3.5] besides the dominant mode diagram [Fig. 1.4; Fig. 2.4; Figs. 3.1, and 3.4] consider two stages of a possible Next Linear e^+e^- Collider: the first with $\sqrt{s} = 500 \text{ GeV}$ and design luminosity 50 fb^{-1} , and the second with $\sqrt{s} = 1 \text{ TeV}$ and luminosity $100\text{-}200 \text{ fb}^{-1}$. We consider the complete set of Feynman diagrams (Figs. 1-3) at tree-level and utilize the helicity formalism for the evaluation of their amplitudes. In the next subsections, we present our results for the case of the different Higgs bosons.

A. Cross section of h^0

In order to illustrate our results on the production of the h^0 Higgs boson, we present graphs of the cross section as functions of A^0 Higgs boson mass m_{A^0} , assuming $m_t = 175$ GeV , $M_t = 500$ GeV and $\tan\beta > 1$ for NLC. Our results are displayed in Fig. 4, for the process at three-body $e^+e^- \rightarrow b\bar{b}h^0$ and for the $e^+e^- \rightarrow (A^0, Z^0) + h^0$ dominant mode.

The total cross section at colliders energies of 500 GeV and 4 different values of the fundamental supersymmetry parameter $\tan\beta$, 6, 10, 30, 50 is of the order of 0.1 pb . We note from this figure, that the effect of the reaction $b\bar{b}h^0$ is light more important than $(A^0, Z^0) + h^0$, for the interval 80 $GeV \leq m_{A^0} \leq 110$ GeV and $\tan\beta = 30, 50$. Nevertheless, there are substantial portions in which the discovery of the h^0 is not possible using either $b\bar{b}h^0$ or $(A^0, Z^0) + h^0$.

For the case of $\sqrt{s} = 1$ TeV , the results of the total cross section of the h^0 are shown in Fig. 8. It is clear from this figure that the contribution of the process $e^+e^- \rightarrow b\bar{b}h^0$ becomes dominant in the interval 80 $GeV \leq m_{A^0} \leq 120$ GeV . However, they could provide important information on the Higgs bosons detection. For instance, we present in the next section tables that illustrate the events number for the process $e^+e^- \rightarrow b\bar{b}h^0$, with $m_{A^0} = 100$ GeV , $\sqrt{s} = (500, 1000)$ GeV and $\tan\beta = 10, 30$.

B. Cross section of H^0

To illustrate our results regarding the detection of the heavy Higgs bosons H^0 , we give the total cross section for both processes $e^+e^- \rightarrow b\bar{b}H^0$ and $e^+e^- \rightarrow (A^0, Z^0) + H^0$ in Fig. 5 for $\sqrt{s} = 500$ GeV .

The total cross section for this case is of the order of 0.01 pb . In this figure, we observed that the effect of incorporate $b\bar{b}H^0$ in the detection of the Higgs boson H^0 is more important than the case of two-body mode $(A^0, Z^0) + H^0$, because $b\bar{b}H^0$ is dominant in all the interval of 100 $GeV \leq m_{A^0} \leq 400$ GeV .

For the case of $\sqrt{s} = 1 \text{ TeV}$, the results are show in Fig. 9. In this case the three-body mode $b\bar{b}H^0$ is light more important that $(A^0, Z^0) + H^0$ for $100 \text{ GeV} \leq m_{A^0} \leq 450 \text{ GeV}$. In the next section are present tables with the events number for $e^+e^- \rightarrow b\bar{b}H^0$.

C. Cross section of A^0

For the pseudoscalar A^0 , it is interesting to consider the production mode in $b\bar{b}A^0$, since it can have large a cross-section due to the fact that the coupling of A^0 with $b\bar{b}$ is directly proportional to $\tan \beta$, thus will always grow with it. In Fig. 6, we present the total cross section for the process of our interest $b\bar{b}A^0$, at $\sqrt{s} = 500 \text{ GeV}$ and $\tan \beta = 6, 10, 30, 50$.

We note that for $\tan \beta = 6, 10, 30, 50$, both the $b\bar{b}A^0$ mode and the $(h^0, H^0) + A^0$ mode have cross sections of the order of 0.1 pb , and for $m_{A^0} > 175 \text{ GeV}$ the process $b\bar{b}A^0$ cover a major region in the parameters space $(m_{A^0}, \tan \beta)$.

On the other hand, if we focus the detection of the A^0 at $\sqrt{s} = 1 \text{ TeV}$, the panorama for its detection is more extensive. The Fig. 10 shows the contours lines in the plane $(\sigma_T - m_{A^0})$, to the production cross section of $b\bar{b}A^0$. The contours for this cross section correspond to $\tan \beta = 6, 10, 30, 50$. The total cross section is of the order of 0.01 pb and the three-body mode $e^+e^- \rightarrow b\bar{b}A^0$ is more important than two-body mode $e^+e^- \rightarrow (h^0, H^0) + A^0$ in all the parameters space.

D. Cross section of H^\pm

Our results for the H^+H^- scalars are displayed in Fig. 7, 11 for the processes at three-body $e^+e^- \rightarrow \tau^-\bar{\nu}_\tau H^+, \tau^+\nu_\tau H^-$ and for the $e^+e^- \rightarrow H^+H^-$ dominant mode.

The total cross section for this reaction with $\sqrt{s} = 500 \text{ GeV}$ and 4 different values of $\tan \beta$, 6, 10, 30, 50 are show in Fig. 7. The cross section is of the order of $\sigma_T \approx 0.1 \text{ pb}$ for $m_{H^\pm} \approx 100 \text{ GeV}$ and $\tan \beta$ large, while for $m_{H^\pm} \approx 200 \text{ GeV}$ is of $\sigma_T \approx 0.01 \text{ pb}$. We can see from this figure that the effect of the reactions $\tau^-\bar{\nu}_\tau H^+$ and $\tau^+\nu_\tau H^-$ is slightly more important than H^+H^- for most of the $(m_{A^0} - \tan \beta)$ parameters space regions. It is precisely

in this curve where the contribution of the processes at three-body is notable. Nevertheless, there are substantial portions of parameters space in which the discovery of the H^\pm is not possible using either H^+H^- or $\tau^-\bar{\nu}_\tau H^+$ and $\tau^+\nu_\tau H^-$.

For the case of $\sqrt{s} = 1 \text{ TeV}$, the results are show in Fig. 11. In both cases ($\tau^-\bar{\nu}_\tau H^+$, $\tau^+\nu_\tau H^-$ and H^+H^-) the curves with $\tan\beta$, 6, 10, 30, 50 given $\sigma_T \approx 0.1 \text{ pb}$ for $m_{H^\pm} \approx 175 \text{ GeV}$. While for $m_{H^\pm} \approx 350 \text{ GeV}$ the cross section drop until 0.001 pb^{-1} for $\tan\beta = 6$. These cross sections are small, however, the contribution of the processes at three-body is slightly more important than the process at two-body. The most important conclusion from this figure is that detection of the charged Higgs bosons will be possible at future e^+e^- colliders.

E. Total Production of the Higgs Bosons

We present in Tables I, II our results for the total production of h^0 , H^0 , A^0 , H^\pm Higgs bosons, taking different values of the center-of-mass energy \sqrt{s} , fundamental supersymmetry parameter $\tan\beta$, luminosity \mathcal{L} , and the mass of the pseudoscalar m_{A^0} . We take the following values representative of the supersymmetric parameters $m_{A^0} = 100 \text{ GeV}$ and $\tan\beta = 10, 30$. From these results we observed a strong dependence of the supersymmetric parameter $\tan\beta$, in particularly for $\tan\beta$ large, as well as, of the center-of-mass energy \sqrt{s} , in the production of the different Higgs bosons (h^0, H^0, A^0, H^\pm). These results make apparent the big importance of investigate the possibility of detecting the Higgs bosons with the reactions at three-body $e^+e^- \rightarrow b\bar{b}h^0(H^0, A^0)$ and $e^+e^- \rightarrow \tau^-\bar{\nu}_\tau H^+, \tau^+\nu_\tau H^-$, at next generation linear e^+e^- colliders.

Total Production of Higgs Bosons	$\mathcal{L}=50 \text{ fb}^{-1}$	
	$\tan \beta = 10$	$\tan \beta = 30$
h^0	1600	1800
H^0	700	470
A^0	900	935
H^+H^-	7000	6500

Table I. Total production of Higgs bosons h^0, H^0, A^0, H^\pm of the MSSM for $\sqrt{s} = 500 \text{ GeV}$ and $m_{A^0} = 100 \text{ GeV}$.

Total Production of Higgs Bosons	$\mathcal{L}=100 \text{ fb}^{-1}$		$\mathcal{L}=200 \text{ fb}^{-1}$	
	$\tan \beta = 10$	$\tan \beta = 30$	$\tan \beta = 10$	$\tan \beta = 30$
h^0	960	1150	1920	2300
H^0	370	220	740	440
A^0	560	615	1120	1230
H^+H^-	4700	4900	9400	9800

Table II. Total production of Higgs bosons h^0, H^0, A^0, H^\pm of the MSSM for $\sqrt{s} = 1 \text{ TeV}$ and $m_{A^0} = 100 \text{ GeV}$.

IV. CONCLUSIONS

In this paper, we have calculated the production of the neutral and charged Higgs bosons in association with b -quarks and with $\tau\nu_\tau$ leptons via the processes $e^+e^- \rightarrow b\bar{b}h$, $h = h^0, H^0, A^0$ and $e^+e^- \rightarrow \tau^-\bar{\nu}_\tau H^+, \tau^+\nu_\tau H^-$ using the helicity formalism. We find that these processes could help to detect the possible neutral and charged Higgs bosons at energies of a possible Next Linear e^+e^- Collider when $\tan \beta$ is large.

In summary, we conclude that the possibilities of detecting or excluding the neutral and charged Higgs bosons (h^0, H^0, A^0, H^\pm) of the Minimal Supersymmetric Standard Model in

the processes $e^+e^- \rightarrow b\bar{b}h$, $h = h^0, H^0, A^0$ and $e^+e^- \rightarrow \tau^-\bar{\nu}_\tau H^+, \tau^+\bar{\nu}_\tau H^-$ are important and in some cases are compared favorably with the dominant mode $e^+e^- \rightarrow (A^0, Z^0) + h$, $h = h^0, H^0, A^0$ and $e^+e^- \rightarrow H^+H^-$ with $\tan\beta$ large. The detection of the Higgs boson will require the use of a future high energy machine like the Next Linear e^+e^- Collider.

Acknowledgments

This work was supported in part by *Consejo Nacional de Ciencia y Tecnología* (CONACYT), *Sistema Nacional de Investigadores* (SNI) (México) and Programa de Mejoramiento al Profesorado (PROMEP). A.G.R. would like to thank the organizers of the Summer School in Particle Physics and Sixth School on non-Accelerator Astroparticle Physics 2001, Trieste Italy for their hospitality. O. A. S. would like to thank CONICET (Argentina).

FIGURE CAPTIONS

Fig. 1 Feynman Diagrams at tree-level for $e^+e^- \rightarrow b\bar{b}h^0$. For $e^+e^- \rightarrow b\bar{b}H^0$ one has to make only the change $\sin \alpha / \cos \beta \rightarrow \cos \alpha / \cos \beta$.

Fig. 2 Feynman Diagrams at tree-level for $e^+e^- \rightarrow b\bar{b}A^0$.

Fig. 3 Feynman Diagrams at tree-level for $e^+e^- \rightarrow \tau^-\bar{\nu}_\tau H^+, \tau^+\nu_\tau H^-$.

Fig. 4 Total Higgs production cross sections $e^+e^- \rightarrow b\bar{b}h^0$ and $e^+e^- \rightarrow (A^0, Z^0) + h^0$ with $\sqrt{s} = 500$ and 4 different values of $\tan \beta$, 6, 10, 30, 50. We have taken $m_t = 175 \text{ GeV}$ and $M_t \sim 500 \text{ GeV}$ and neglected squark mixing.

Fig. 5 Same as in Fig. 4, but for $e^+e^- \rightarrow b\bar{b}H^0$ and $e^+e^- \rightarrow (A^0, Z^0) + H^0$.

Fig. 6 Same as in Fig. 4, but for $e^+e^- \rightarrow b\bar{b}A^0$ and $e^+e^- \rightarrow (h^0, H^0) + A^0$.

Fig. 7 Same as in Fig. 4, but for $e^+e^- \rightarrow \tau^-\bar{\nu}_\tau H^+, \tau^+\nu_\tau H^-$ and $e^+e^- \rightarrow H^+H^-$.

Fig. 8 Total Higgs production cross sections for $\sqrt{s} = 1 \text{ TeV}$ and 4 different values of $\tan \beta$, 6, 10, 30, 50. We have taken $m_t = 175 \text{ GeV}$, $M_t \sim 500 \text{ GeV}$ and neglected squark mixing. We display contours for $e^+e^- \rightarrow b\bar{b}h^0$ and $e^+e^- \rightarrow (A^0, Z^0) + h^0$, in the parameters space $(\sigma_T - m_{A^0})$.

Fig. 9 Same as in Fig. 8, but for $e^+e^- \rightarrow b\bar{b}H^0$ and $e^+e^- \rightarrow (A^0, Z^0) + H^0$.

Fig. 10 Same as in Fig. 8, but for $e^+e^- \rightarrow b\bar{b}A^0$ and $e^+e^- \rightarrow (h^0, H^0) + A^0$.

Fig. 11 Same as in Fig. 8, but for $e^+e^- \rightarrow \tau^-\bar{\nu}_\tau H^+, \tau^+\nu_\tau H^-$ and $e^+e^- \rightarrow H^+H^-$.

REFERENCES

- [1] P. W. Higgs, Phys. Lett. **12**, (1964) 132; P. W. Higgs, Phys. Rev. Lett. **13**, (1964) 508; P. W. Higgs, Phys. Rev. Lett. **145**, (1966) 1156; F. Englert, R. Brout, Phys. Rev. Lett. **13**, (1964) 321; G. S. Guralnik, C. S. Hagen, T. W. B. Kibble, Phys. Rev. Lett. **13** (1964), 585.
- [2] S. Weinberg, Phys. Rev. Lett. **19**, (1967) 1264; A. Salam, in *Elementary Particle Theory*, ed. N. Southholm (Almquist and Wiksell, Stockholm, 1968), p.367; S.L. Glashow, Nucl. Phys. **22**, (1967) 257.
- [3] H. P. Nilles, Phys. Rep. **110**, (1984) 1; H. Haber and G. L. Kane, Phys. Rep. **117**, (1985) 75.
- [4] J. F. Gunion and H. E. Haber, Nucl. Phys. **B272**, (1986) 1; Nucl. Phys. **B278**, (1986) 449; Nucl. Phys. B307, (1988) 445; erratum *ibid.* **B402**, (1993) 567.
- [5] S.P. Li and M. Sher, phys. Lett. **B149**, (1984) 339; J. F. Gunion and A. Turski, Phys. Rev. **D39**, (1989) 2701; **40**, (1989) 2325; **40**, (1989) 2333; Y. Okada *et al.* Prog. Theor. Phys. **85**, (1991) 1; H. Haber and R. Hempfling, Phys. Rev. Lett. **66**, (1991) 1815; J. Ellis *et al.*, Phys. Lett. **B257**, (1991) 83; M. Dress and M. N. Nojiri, Phys. Rev. **D45**, (1992) 2482; M. A. Diaz and H. E. Haber, Phys. Rev. **D45**, (1992) 4246; D. M. Pierce, A. Papadopoulos and S. Jonhson, Phys. Rev. Lett. **68**, (1992) 3678; P. H. Chankowski, S. Poporski and J. Rosiek, Phys. Lett. **B274**, (1992) 191; A. Yamada, Mod. Phys. Lett. **A7**, (1992) 2877.
- [6] Particle Data Group, Review of Particle Physics, Eur. Phys. J. **C15**, (2000) 1.
- [7] S. Komamiya, Phys. Rev. **D38**, (1988) 2158.
- [8] For a recent review see J. Gunion, H. Haber, G. Kane and S. Dowson, *The Higgs Hunter's Guide* (Addison-Wesley, Reading, MA, 1990).
- [9] P. Janot, Orsay Report No. LAL 91-61, 1991 (unpublished); J-F Grivas, Orsay Report

No. LAL 91-63, 1991 (unpublished) A. Brignole, J. Ellis, J. F. Gunion, M. Guzzo, F. Olnes, G. Ridolfi, L. Roszkowski and F. Zwirner, *in e^+e^- Collision at 500 GeV: The Physics Potential*, Munich, Annecy, Hamburg Workshop, DESY 92-123A, DESY 92-123B, DESY 93-123C, ed. P. Zerwas, p. 613; A. Djouadi, J. Kalinowski, P. M. Zerwas, *ibid.*; p.83 and Z. Phys. **C57**, (1993) 56; and references therein; *Physics and Technology of the Next Linear*: a Report Submitted to Snowmass 1996, BNL 52-502, FNAL-PUB-96/112, LBNL-PUB-5425,SLAC Report 485, UCRL-JD-124160.

[10] M. Carena and P. M. Zerwas, Working Group, hep-ph/9602250, and references therein; S. Moretti and W. J. Stirling, Phys. Lett. **B347**, (1995) 291; Erratum, *ibidem* **B366**, (1996) 451. J. F. Gunion, *Detection and Studying Higgs Bosons*, hep-ph/9705282, UCD-97-13, 1997;

[11] Andre Sopczak, Z. Phys. **C65**, (1995) 449; A. Sopczak, hep-ph/9712283, IEKP-KA/97-14, 1997; Stefano Moretti and Kosuke Odagiri, hep-ph/9612367; S. Moretti and K. Odagiri, Eur. Phys. J. **C1**, (1998) 633; E. Accomando, et al. Phys. Rep. **299**, (1998) 1.

[12] A. Djouadi, J. Kalinowski and P. M. Zerwas, Mod. Phys. Lett. **A7**, (1992) 1765; Z. Phys. **C54**, (1992) 255; S. Dittmaier, M. Krämer, Y. Liao, M. Spira and P. M. Zerwas, Phys. Lett. **B441**, (1998) 383, *ibid.* **B478**, (2000) 274; S. Dawson and L. Reina, Phys. Rev. **D57**, (1998) 5851, *ibid.* **D59**, (1999) 054012, *ibid.* **D60**, (1999) 015003.

[13] U. Cotti, A. Gutiérrez-Rodríguez, A. Rosado and O. A. Sampayo, Phys. Rev. **D59**, (1999) 095011.

[14] A. Gutiérrez-Rodríguez and O. A. Sampayo, Phys. Rev. **D62**, (2000) 055004; A. Gutiérrez-Rodríguez and O. A. Sampayo, hep-ph/9911361; A. Gutiérrez-Rodríguez, M. A. Hernández-Ruiz and O. A. Sampayo, hep-ph/0005050.

[15] S. Kanemura, S. Moretti and K. Odagiri, hep-ph/0101354; Shinya Kanemura, Stefano Moretti, Kosuke Odagiri, hep-ph/0012030.

[16] NLC ZDR Desing Group and the NLC Physics Working Group, S. Kuhlman *et al.*, *Physics and Technology of the Next Linear Collider*, hep-ex/9605011.

[17] The NLC Design Group, C. Adolphsen *et al.* Zeroth-Order Design Report for the *Next Linear Collider*, LBNL-PUB-5424, SLAC Report No. 474, UCRL-ID-124161 (1996).

[18] JLC Group, JLC-I, KEK Report No. 92-16, Tsukuba (1992).

[19] Howard E. Haber, *Proceedings of the 21st SLAC Summer Institute on Particle Physics: Spin Structure in High Energy Process* SLAC, Stanford, CA, 26 July-6 August 1993.

[20] Zhan Xu, Da-Hua Zhang and Lee Chang, Nucl. Phys. **B291**, (1987) 392.

[21] J. Werle, *Relativistic Theory of Reactions* (North-Holland, Amsterdam, 19976); A. D. Martin and T. D. Spearman, *Elementary Particle Physics* (North-Holland, Amsterdam, 1970); S. U. Chung, *Spin Formalism*, CERN Yellow Report 71-8 (1971); Martin L. Perl, *High Energy Hadron Physics* (John Wiley Sons, New York, 1974).

[22] H. Pilkum, *The Interactions of Hadrons* (North-Holland, Amsterdam, 1967).

[23] Peter A. Carruthers, *Spin and Isospin in Particle Physics* (Gordon and Breach, New York, 1971); M. D. Scadron, *Advanced Quantum Theory* (Springer-Verlag, Berlin, 1991).

[24] M. L. Mangano and S. J. Parke, Phys. Rep. **200**, (1991) 301.

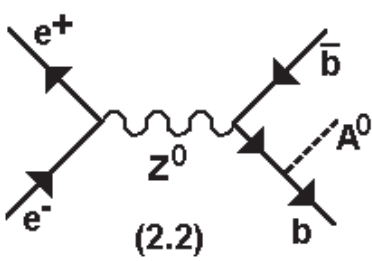
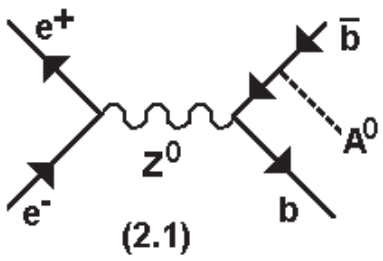
[25] F. A. Berends, P. H. Daverveldt and R. Kleiss, Nucl. Phys. **B253**, (1985) 441; R. Kleiss and W. J. Stirling, Nucl. Phys. **B262**, (1985) 235; C. Mana and M. Martinez, Nucl. Phys. **B278**, (1987) 601.

[26] J. Lorenzo Díaz-Cruz, Hong-Jian He, Tim Tai, C.-P. Yuan, Phys. Rev. Lett. **80**, (1998) 4641; M. Carena, S. Mrenna and C. E. M. Wagner, *MSSM Higgs Boson Phenomenology at the Tevatron Collider*, hep-ph/9808312v2; C. Balázs, J. Lorenzo Díaz-Cruz, Hong-Jian He, Tim Tai, C.-P. Yuan, *Probing Higgs Bosons with Large Bottom Yukawa Coupling at Hadron Colliders*, hep-ph/9807349.

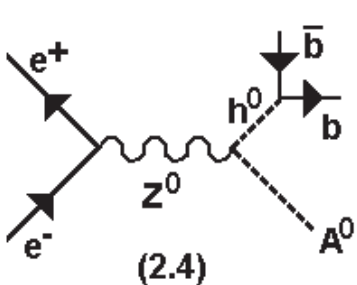
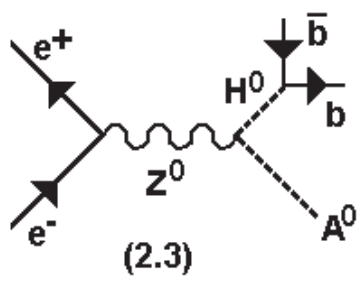
[27] A. C. Hearn, *REDUCE User's Manual*, version 3.2 (Rand Publ. CP78 Rev. 4/85, Santa Monica, CA. 1985); H. Strubbe, *Comput. Phys. Commun.* **8**, (1974) 1.

[28] P. De Causmaecker, R. Gastmans, W. Troost and T. T. Wu, *Phys. Lett.* **B105**, (1981) 215; P. De Causmaecker, R. Gastmans, W. Troost and T. T. Wu, *Nucl. Phys.* **B206**, (1982) 53; F. A. Berends, R. Kleiss, P. De Causmaecker, R. Gastmans, W. Troost and T. T. Wu, *Nucl. Phys.* **B206**, (1982) 61; D. Dankaert, P. De Causmaecker, R. Gastmans, W. Troost and T. T. Wu, *Phys. Lett.* **B114**, (1982) 203; F. A. Berends, P. De Causmaecker, R. Gastmans, R. Kleiss, W. Troost and T. T. Wu, *Nucl. Phys.* **B239**, (1984) 382; F. A. Berends, P. De Causmaecker, R. Gastmans, R. Kleiss, W. Troost and T. T. Wu, *Nucl. Phys.* **B239**, (1984) 395; F. A. Berends, P. De Causmaecker, R. Gastmans, R. Kleiss, W. Troost and T. T. Wu, *Nucl. Phys.* **B264**, (1986) 234; F. A. Berends, P. De Causmaecker, R. Gastmans, R. Kleiss, W. Troost and T. T. Wu, *Nucl. Phys.* **B264**, (1986) 265.

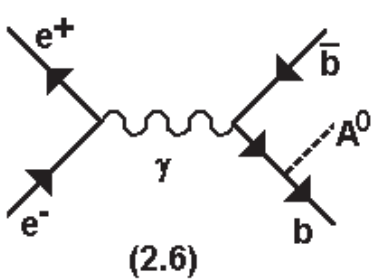
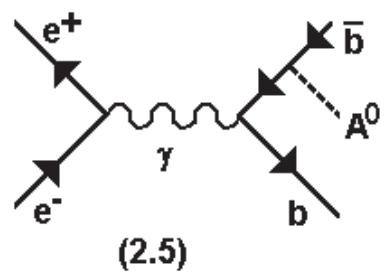
[29] R. Kleiss, W. J. Stirling and S. D. Ellis, *Comput. Phys. Commun.* **40** (1986) 359.



A^0



A^0



A^0

Fig. 2

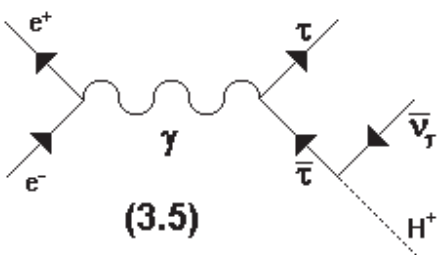
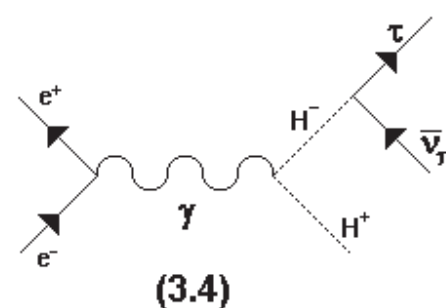
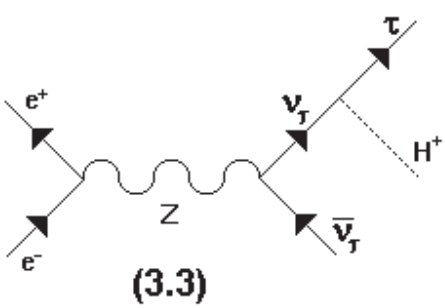
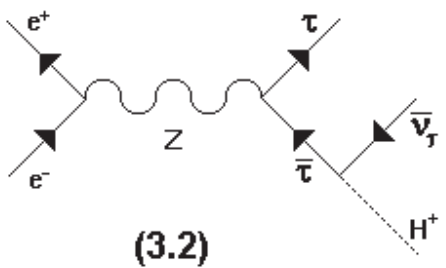
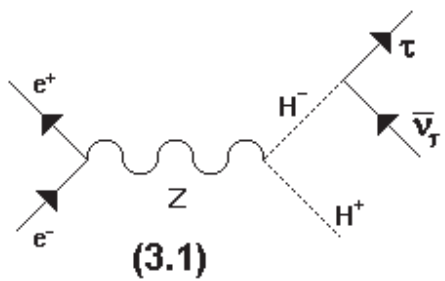


Fig. 3

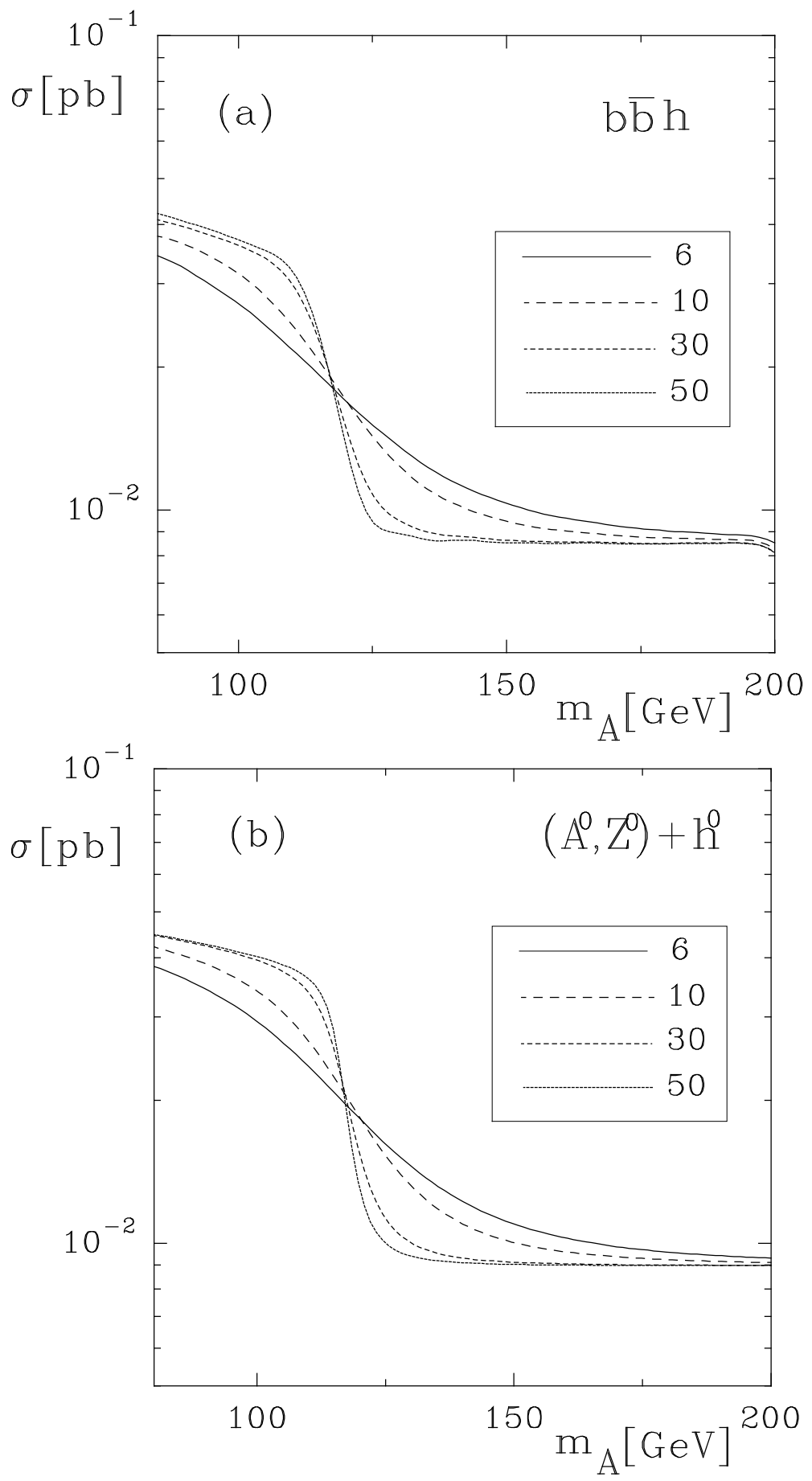
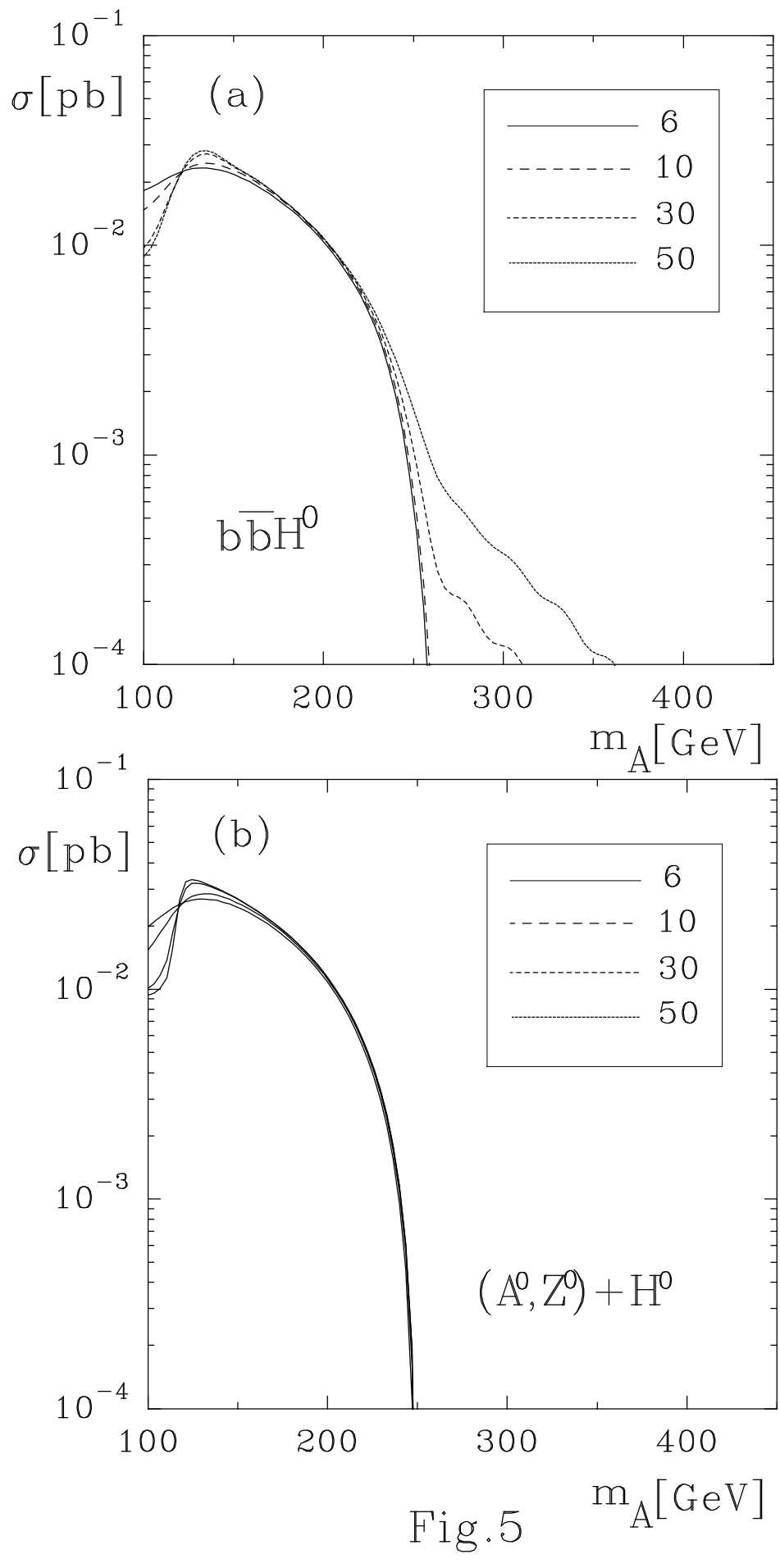


Fig. 4



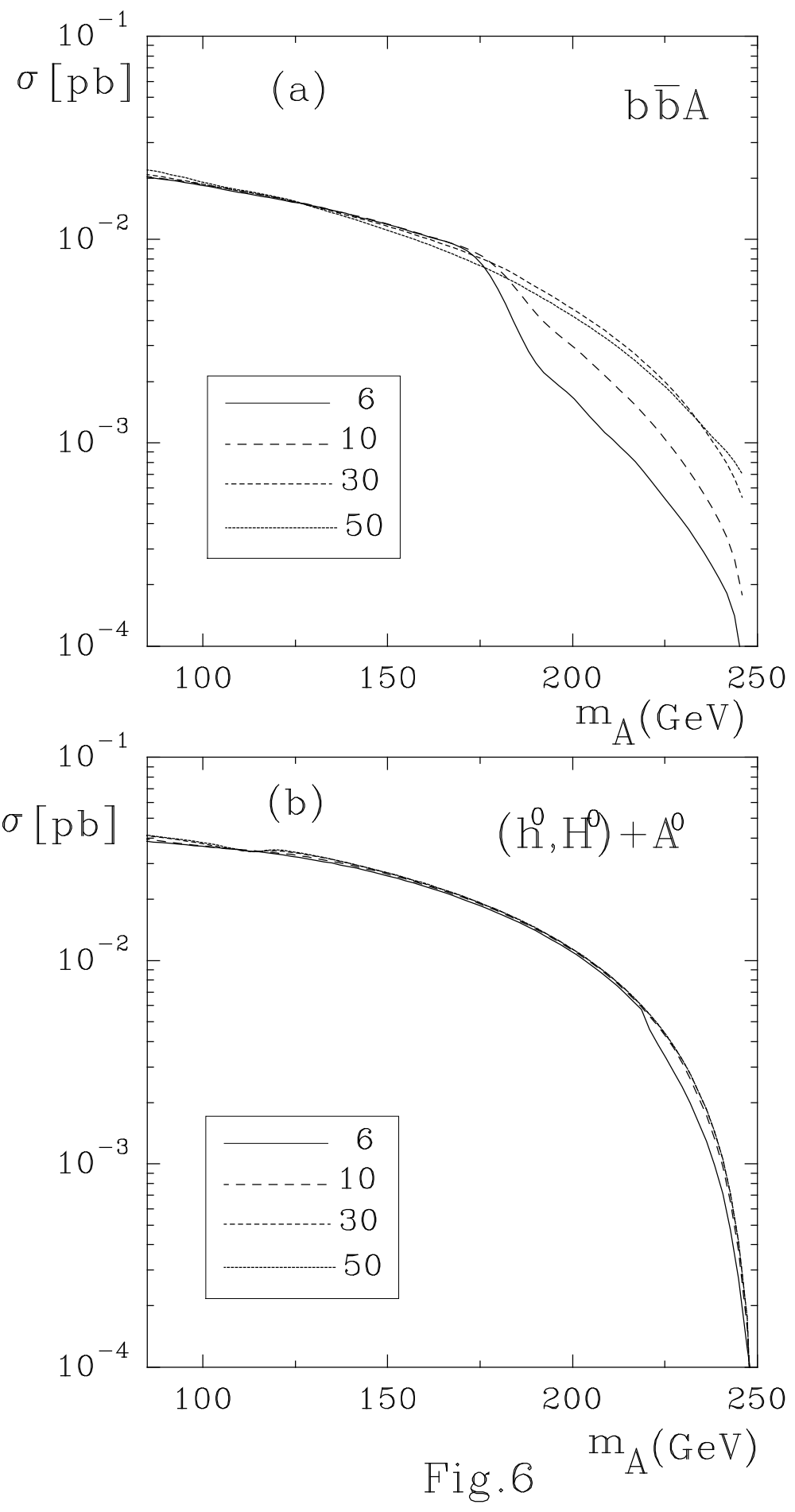


Fig.6

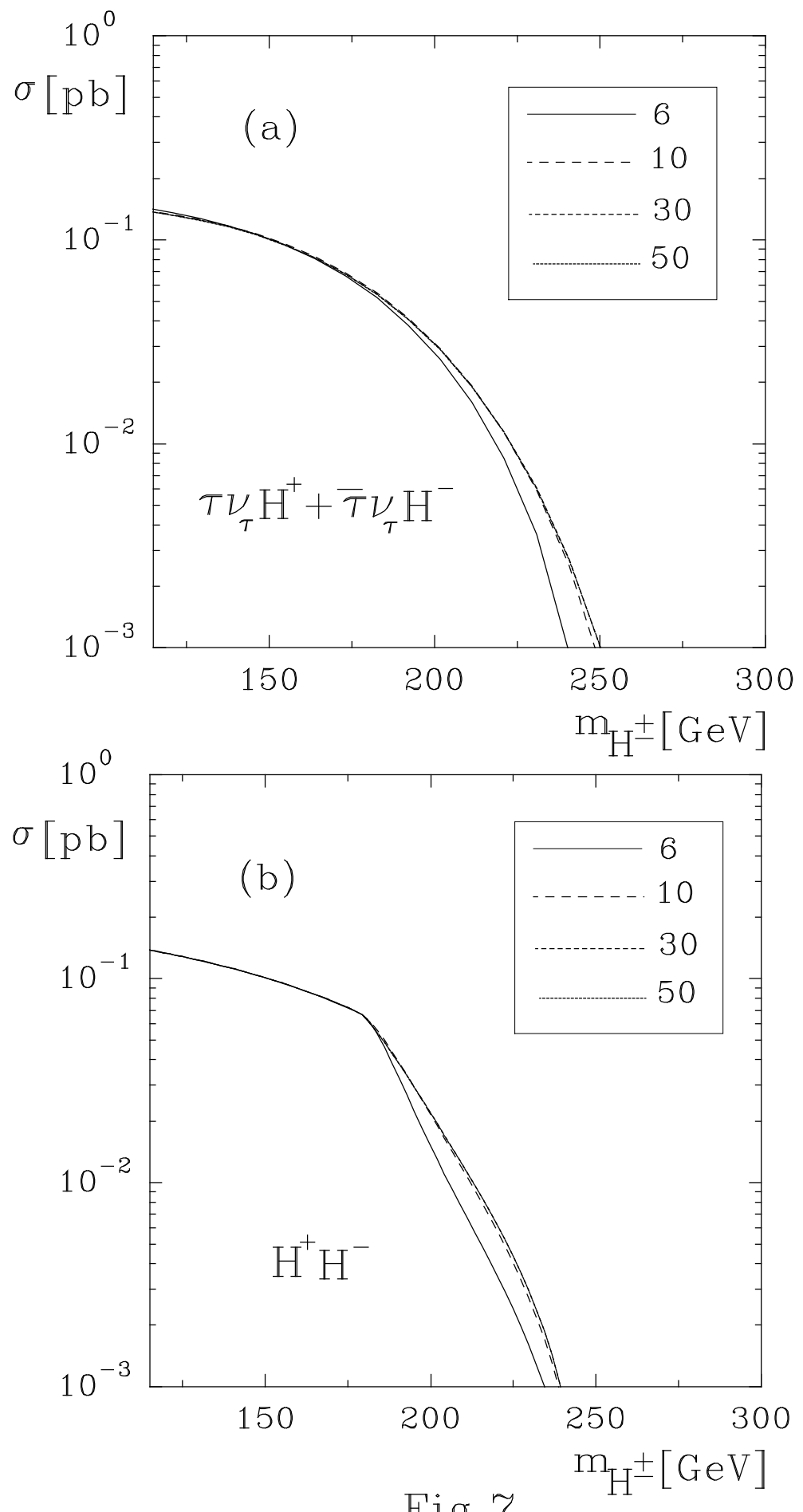


Fig. 7

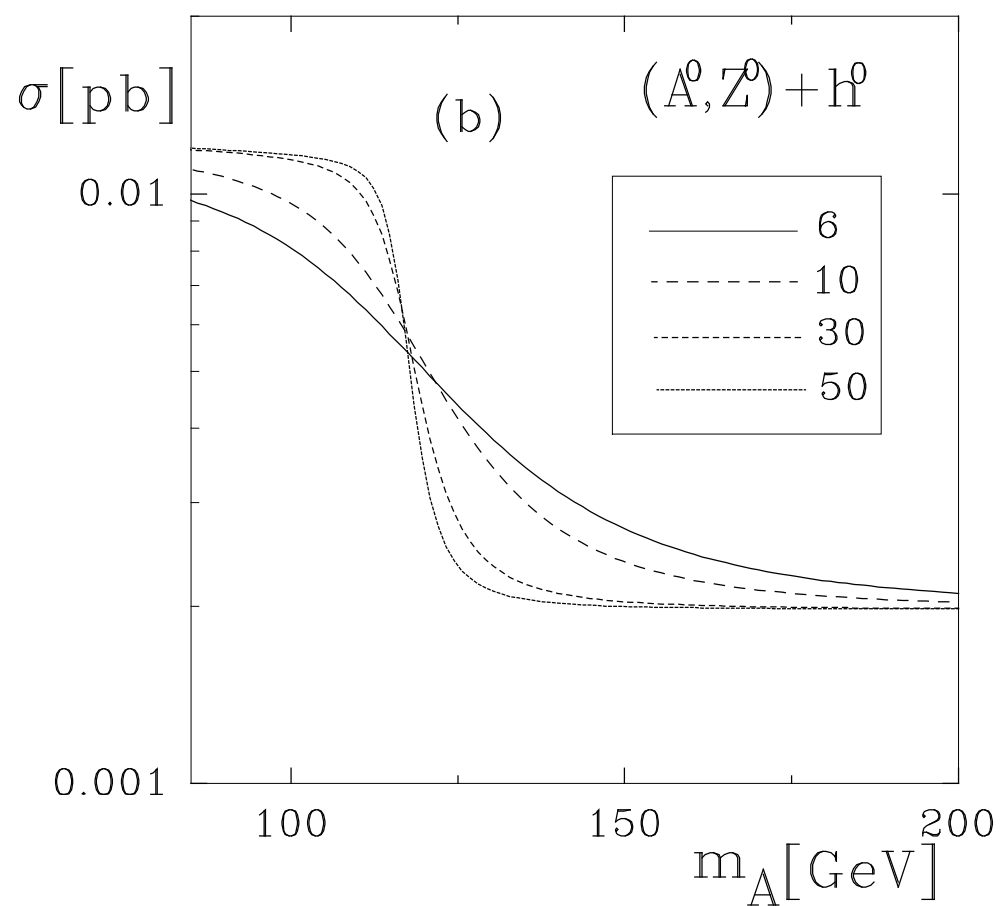
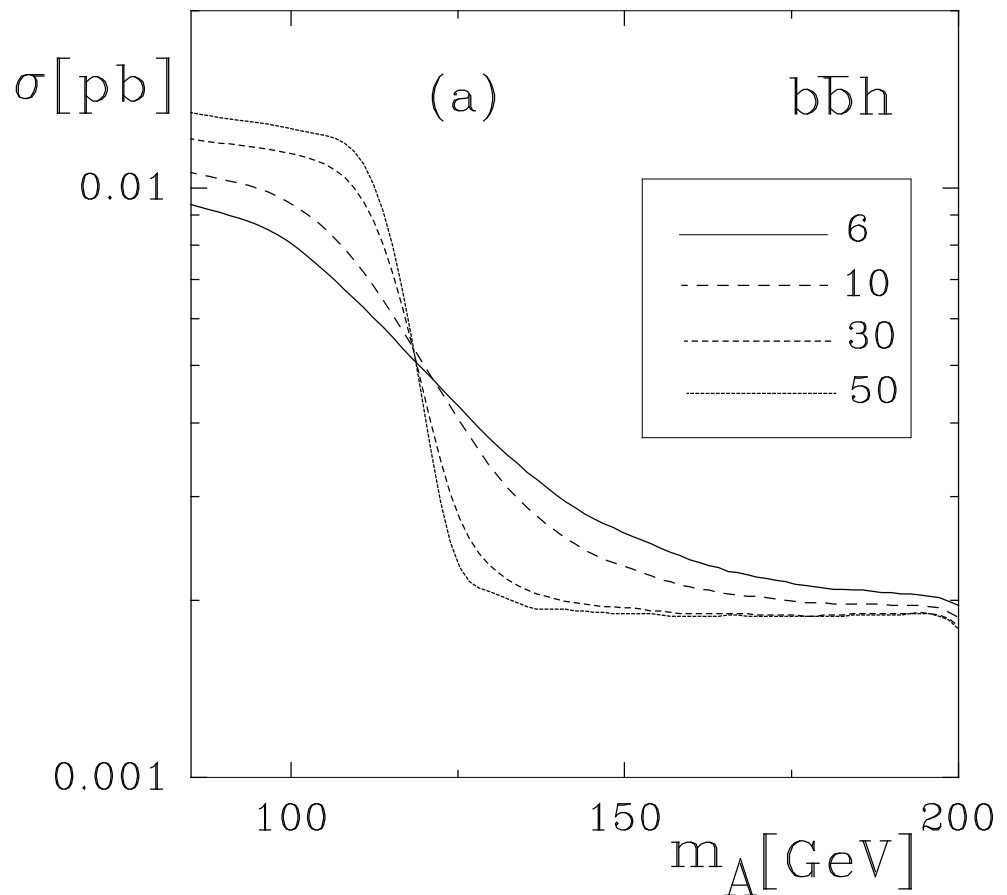


Fig.8

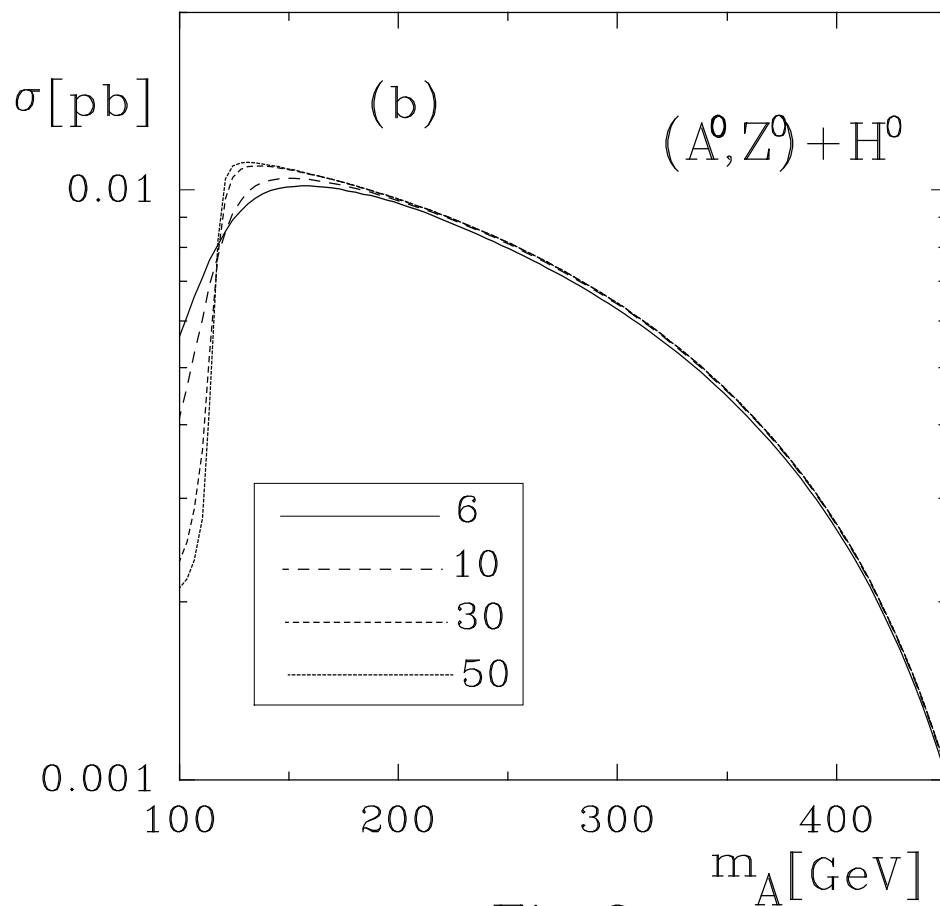
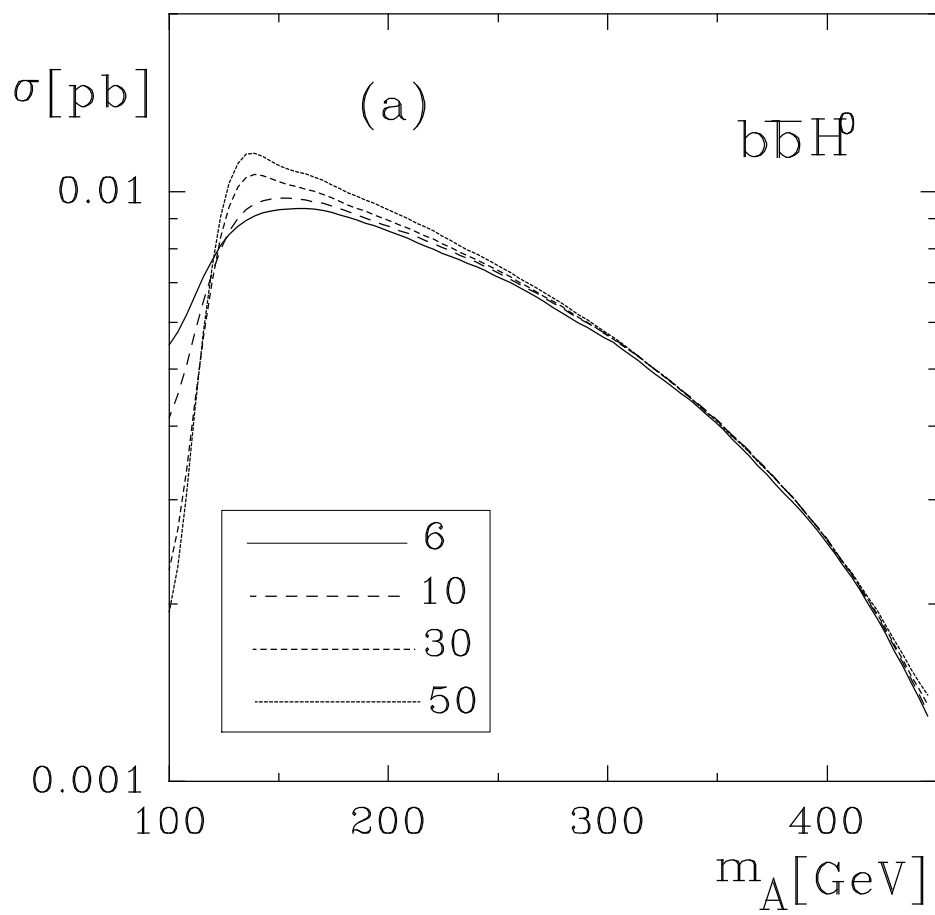
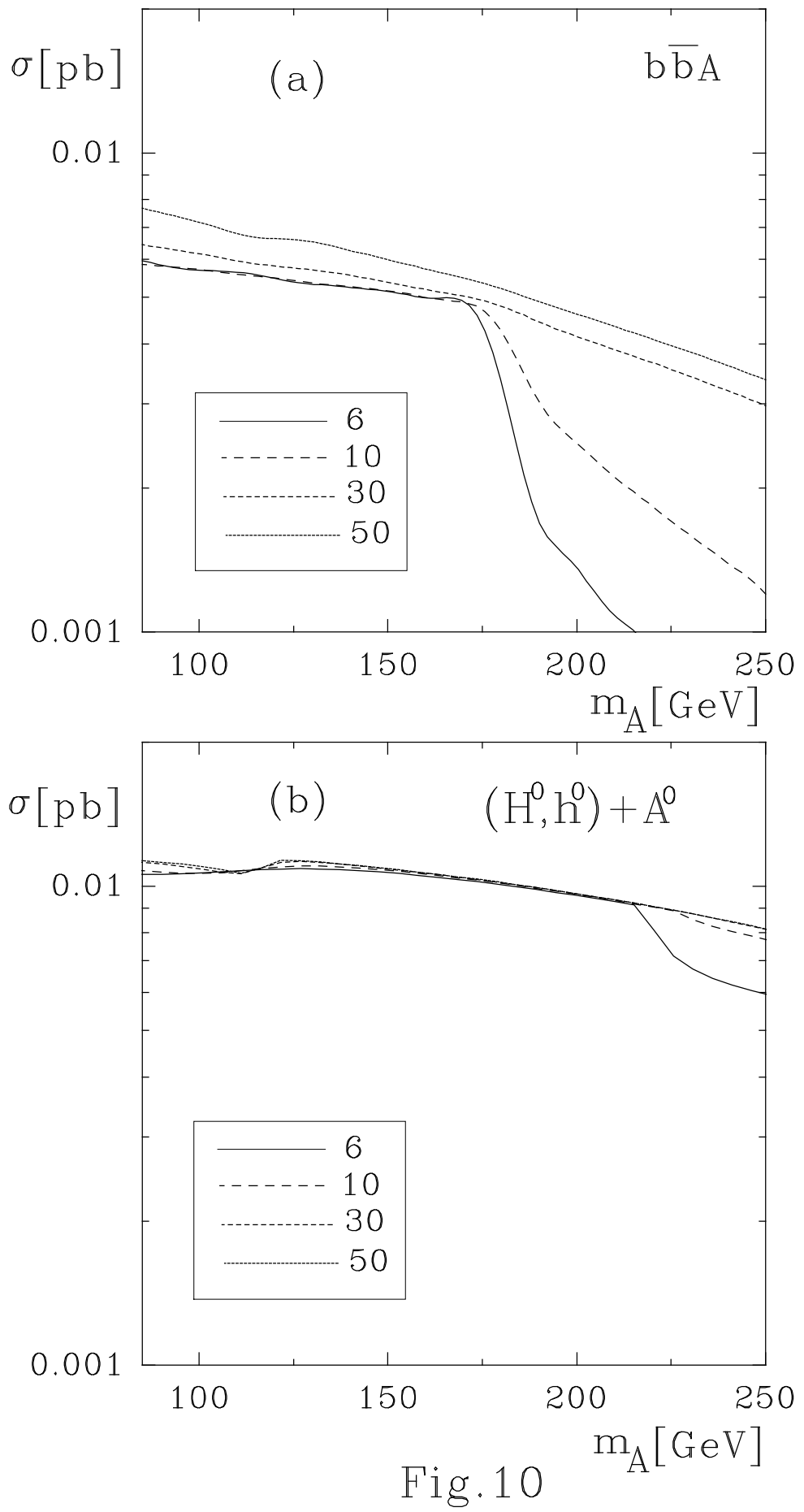


Fig.9



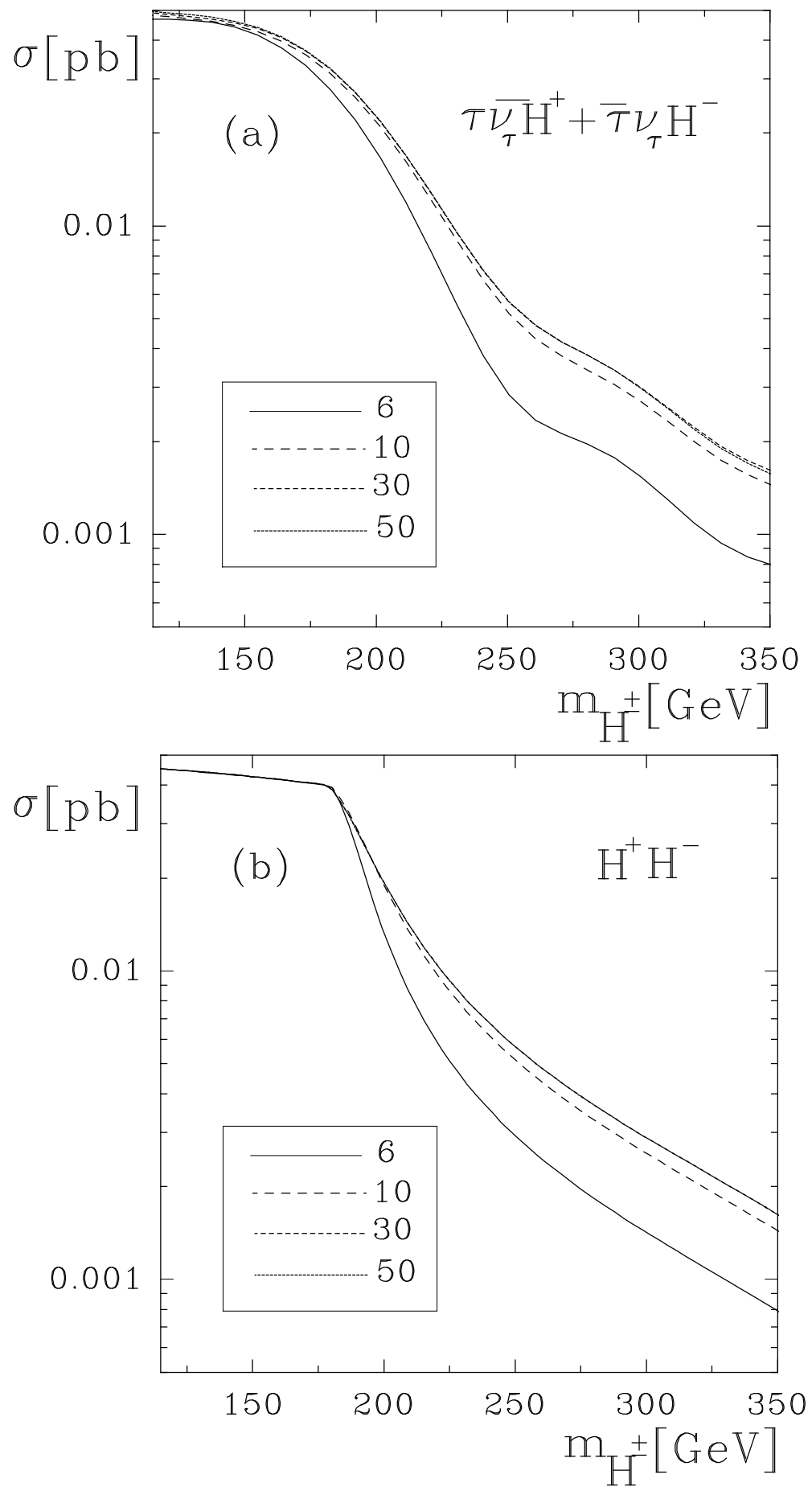


Fig. 11